CCCARD2014-004

Thermalhydraulics and Safety-Related Experiments in support of the Canadian SCWR Concept Development

Laurence K.H. Leung
Atomic Energy of Canada Limited, Chalk River, Ontario, Canada K0J 1P0
leungl@aecl.ca

Abstract

A Canadian National Program has been established for R&D in various technology areas in support of the Canadian Super-Critical Water-cooled Reactor (SCWR) concept development. The thermalhydraulics and safety projects in the National Program had led to the establishment of infrastructure and capabilities at universities. Current projects focus on the applied research to provide relevant experimental databases for developing or validating prediction methods and analytical toolsets. Several experimental projects are currently being carried out to obtain heat-transfer data with annuli, 3-rod assembly, and 4-rod assembly in refrigerant-134a flow, carbon dioxide flow, and water flow, respectively, and blow-down and natural-circulation data with tubes in water and carbon dioxide flow, respectively. Key scopes of these experimental projects are described. Experimental data obtained from these projects are presented.

1. Introduction

Canada is participating in research for the development of the Super-Critical Water-cooled Reactor (SCWR); one of the Gen-IV nuclear-reactor systems in the Generation-IV International Forum (or GIF). The Canadian effort focuses mainly on the pressure-tube type of the SCWR, which is a natural extension of the existing CANDU® reactor. A Canadian national program has been established to support the development of the Canadian SCWR with participation of Canadian universities, federal laboratories and agencies, and Atomic Energy of Canada Limited (AECL) [1]. In addition, AECL collaborates bilaterally with several Chinese universities to accelerate the R&D program. The Canadian Gen-IV National Program is separated into two phases, with the first phase focusing on establishing infrastructure for supercritical fluid research in Canada and the second phase aiming at generating relevant experimental data in support of the concept development.

Thermal-hydraulics analyses are required in support of fuel and core designs for SCWRs. There is no phase change above the critical pressure of water and thus, supercritical water can be regarded as a single-phase fluid. However, it is widely recognized that the thermophysical properties of supercritical water undergo drastic variations at the pseudo-critical temperature. These drastic variations lead to unusual heat-transfer phenomena for supercritical water compare to single-phase fluid with constant properties. This issue is more complicated in fuel assemblies where large imbalances in flow and enthalpy can be encountered.

The thermalhydraulics and safety projects cover experimental and analytical studies. The objective of this paper is to summarize the thermalhydraulics and safety-related experiments in support of the development of the Canadian SCWR concept.

2. Heat Transfer Experiments with Supercritical Flow

Experimental data on heat transfer in supercritical flow are required for the fuel-assembly concept to support the core design and safety analysis. Performing experiments using a full-scale fuel assembly is premature at this stage since both the core and fuel designs are still in the conceptual phase. In most cases, tube-data-based heat-transfer correlations are applied in the analyses. This approach introduces large uncertainty in the heat-transfer predictions due to the neglect of the separate effects encountered in fuel assemblies.

Applying analytical tools is an alternate approach to establish heat-transfer characteristics for the fuel-assembly concept. These analytical tools include subchannel codes and computational fluid dynamic (CFD) codes. In most cases, tube-data-based heat-transfer correlations are required for implementation into subchannel codes. Experimental data for tubes and annuli are applied for validating CFD predictions and/or establishing the appropriate model.

The heat-transfer experiments in support of the Canadian SCWR development are performed with water, carbon dioxide, covering simple test sections and bundle subassemblies. Test sections with simple geometry, such as tubes and annuli, were used for commissioning and fundamental studies. Bundle subassemblies with either three, four or seven rods have been constructed and are being tested in, respectively, carbon dioxide, water, or refrigerant-134a flow.

2.1 Supercritical Water Heat-Transfer Test

In support of the development of the Canadian SCWR concept, Atomic Energy of Canada Limited is collaborating with Xi'an Jiaotong University in performing heat transfer experiments of supercritical water using annuli [7] and a 2×2 rod-bundle simulator. These experiments generated data for examining various separate effects and validating analytical tools.

2.1.1 Annuli Tests

The annular test sections consisted of an inner heated tube and an outer unheated shroud; both were made of stainless-steel tubes. The inner tube has an outer diameter of 8 mm and a wall thickness of 1.5 mm. It was heated with electric current over a heated length of 2 meters. Thermocouples were installed inside the inner heated tube to measure the inner-wall temperature. Two outer tubes having inner diameters of 16 and 20 mm, with a wall thickness of 2 mm, were tested to examine the effect of gap size (or flow area) on supercritical heat transfer.

The inner heated tube is helically wrapped with a string of ceramic tubes with the diameter of 3 mm to simulate a fuel pin with a helical wire-wrapped spacer. One pitch of the helical spacer is 50 mm and the full length of the helical wire-wrapped spacer along the inner pipe is 100 mm, that is, two pitches at a spiral angle of 45^{o}. The helical wire-wrapped spacer was installed only at the first upstream thermocouple location (i.e., other locations in the heated tube were not equipped with spacers). Figure 1 illustrates schematically the annulus test section design, locations of thermocouples, and the

spacer. The test section was installed vertically in the loop and tested with an upward flow of water. Inlet and outlet fluid-temperatures, outlet pressure, and pressure drop over the test section were measured.

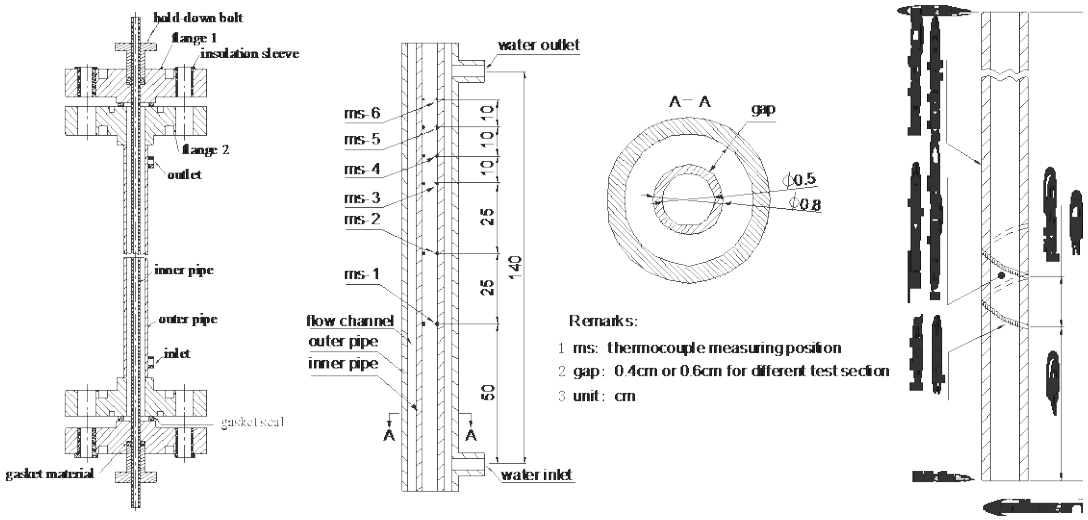

Figure 1: Schematic Diagram of the Annulus Test Section

Wall temperature measurements have been obtained over a range of mass fluxes and heat fluxes at outlet pressures of 23, 25 and 28 MPa. Figure 2 illustrates variations of wall-temperature measurements with local enthalpy and heat flux at the mass flux of 1000 kg/(m^2s) and the pressure of 25 MPa. The wall temperature increases with increasing fluid enthalpy and increasing heat flux. This increasing trend becomes relatively gradual near the pseudo-critical enthalpy at low heat fluxes. It follows closely the variation of the bulk-fluid temperature (t_b). The gradual increasing trend diminishes with increasing heat flux.

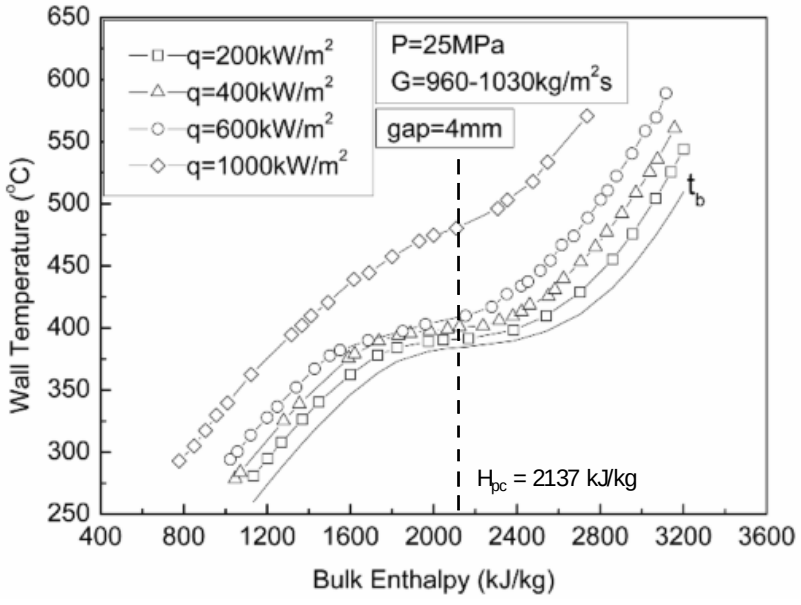

Figure 2: Wall Temperature Measurements with Vertical Upflow of Supercritical Water inside an Annulus Test Section

Figure 3 illustrates the corresponding heat transfer coefficient calculated from the wall-temperature measurements. The heat-transfer coefficient generally increases with increasing enthalpy in the low-enthalpy region. A peak heat-transfer coefficient is observed near the pseudo-critical point (following closely the variation of the specific heat). The peak appears shifting to a lower enthalpy at the heat flux of 1000 kW/m^2. Beyond the peak, the heat-transfer coefficient decreases with increasing enthalpy. At the heat flux of 1000 kW/m^2, the heat-transfer coefficient is significantly lower than those of other heat fluxes at the pseudo-critical point. This is often referred to as the deteriorated heat-transfer region. Parametric trends of heat-transfer coefficient have been examined with mass flux and pressure, in addition to enthalpy and heat flux.

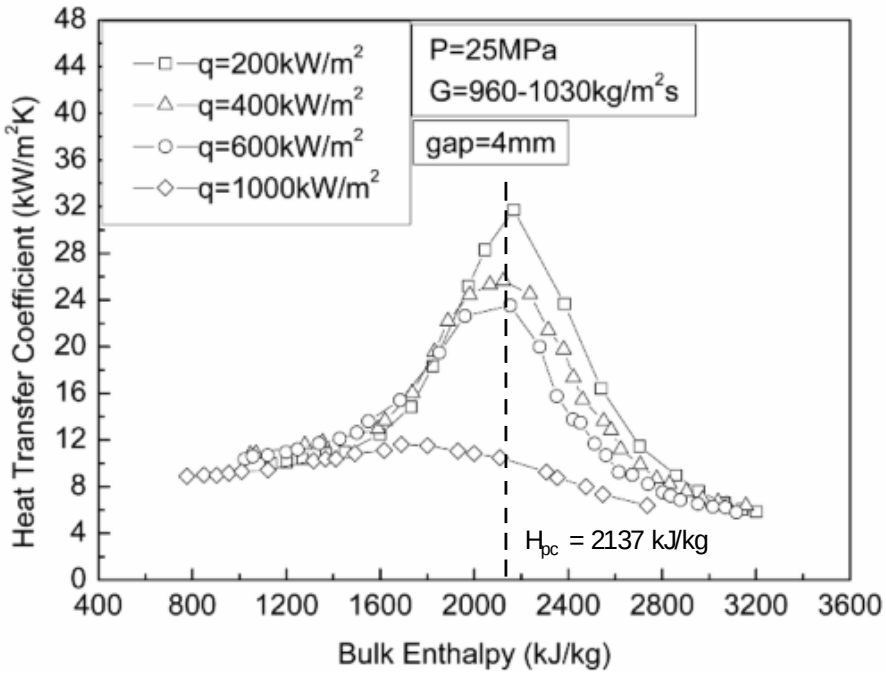

Figure 3: Heat-Transfer Coefficients with Vertical Upflow of Supercritical Water inside an Annulus Test Section

As described above (see Figure 1), the inner heated tube was equipped with a wrap-around ceramic spacer at the location of the first set of thermocouples (i.e., ms$_1$). Figure 4 illustrates the variation of heat-transfer coefficient, evaluated from surface-temperature measurement, with bulk-fluid enthalpy. The largest heat-transfer coefficient is observed at the spacer location (i.e., ms$_1$), and the lowest at the location further downstream of the spacer near the channel exit (i.e., ms$_6$). The reduction in heat-transfer coefficient is sharp at locations close to the spacer, but diminishes gradually with increasing distance from the spacer. Furthermore, the peak heat-transfer coefficient shifts to low enthalpy at locations further away from the spacer.

The effect of gap size (or flow area) on heat transfer has been examined through comparison of experimental heat-transfer coefficients obtained with the 16- and 20-mm outer unheated tubes (4- and

6-mm gap sizes, respectively). Figure 5 illustrates variations of heat-transfer coefficient with bulk-fluid enthalpy for two sets of flow conditions and heat fluxes in the two tested annuli. The heat-transfer coefficient is larger for the 6-mm gap-size channel than the 4-mm gap-size channel at similar flow conditions and heat fluxes. Differences in heat-transfer coefficient become small at mass flux of 400 kg/(m^2s) and heat flux of 600 kW/m^2. This seems to indicate a diminishing effect of gap size.

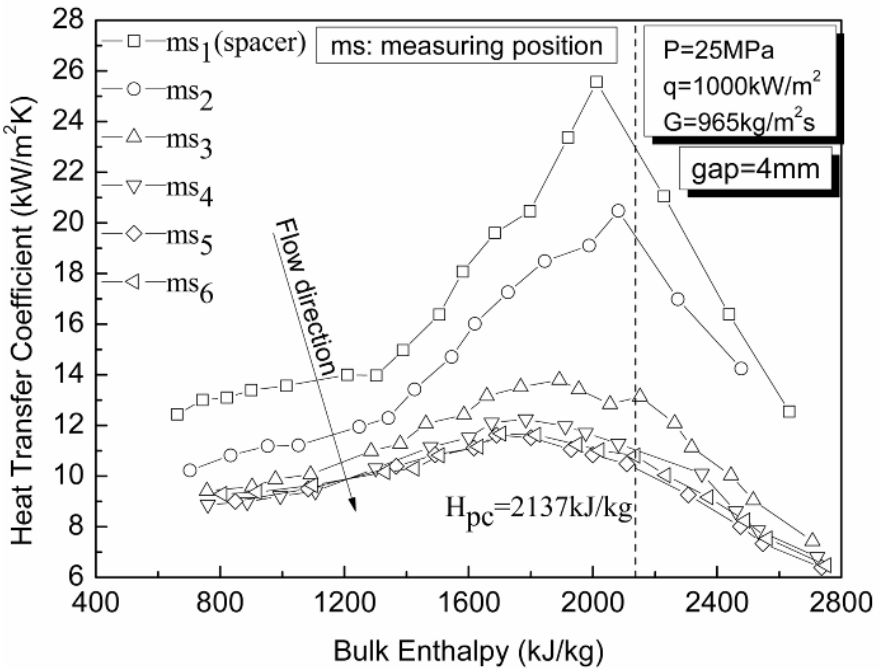

Figure 4: Effect of Spacer on Supercritical Heat Transfer.

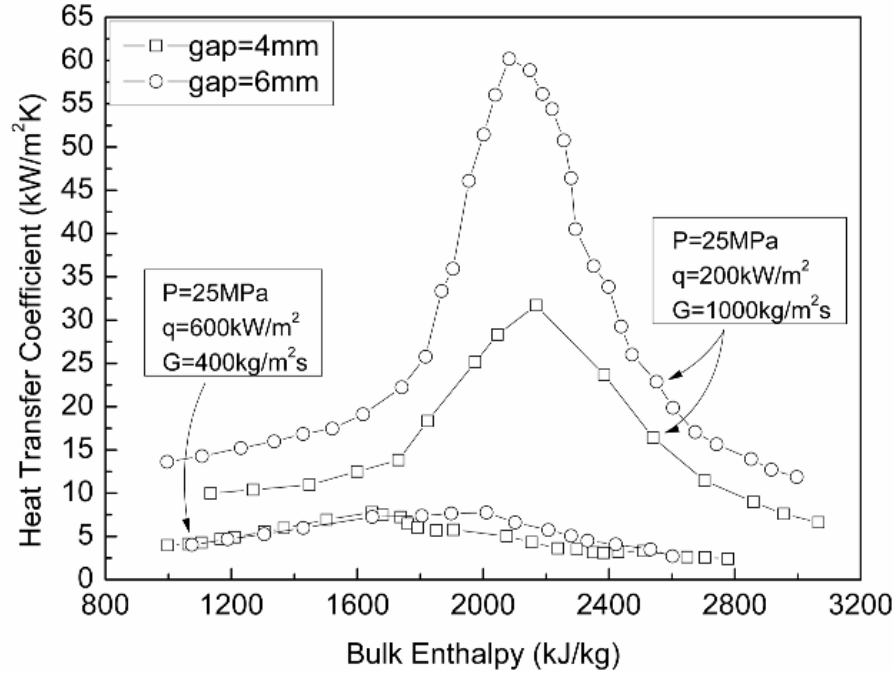

Figure 5: Effect of Gap Size (or Flow Area) on Supercritical Heat Transfer.

2.1.2 2x2 Bundle Tests

Heat transfer experiments have been performed with supercritical water through a 2×2 bundle to provide circumferential wall-temperature measurements around the heated rods. These experiments consist of two phases: the first phase focuses on the bundle configuration with no spacing device (i.e., bare bundle) and the second phase on the bundle configuration with the wrapped-wire spacers. Based on test results observed in annuli and bundles from previous studies, wall-temperature measurements obtained in the first phase are anticipated to be higher than those in the second phase (due to the enhancement effect of the wrapped-wire spacers).

Figure 6 illustrates the overall configuration of the test section geometry. The test section in the heated region consisted of an outer unheated stainless steel tube, which served as the pressure boundary, and a square insulator (20.32×20.32 mm^2) with round corners and electrically isolating the heated bundle from the outer tube. The outer tube was thermally insulated to minimize heat loss to the environment. The 2×2 rod bundle consisted of four stainless-steel (SS-304) tubes, each having an outer diameter of 8 mm and a wall thickness of 1.5 mm. Each end of the tube was plated with a silver coating for electric conduction; the middle region of the tube was not plated resulting in a heated section of 600 mm. The gap between two heated rods was maintained at 1.44 mm, and the gap between the heated rod and the rounded corner of the square ceramic insulator was also maintained at 1.44 mm.

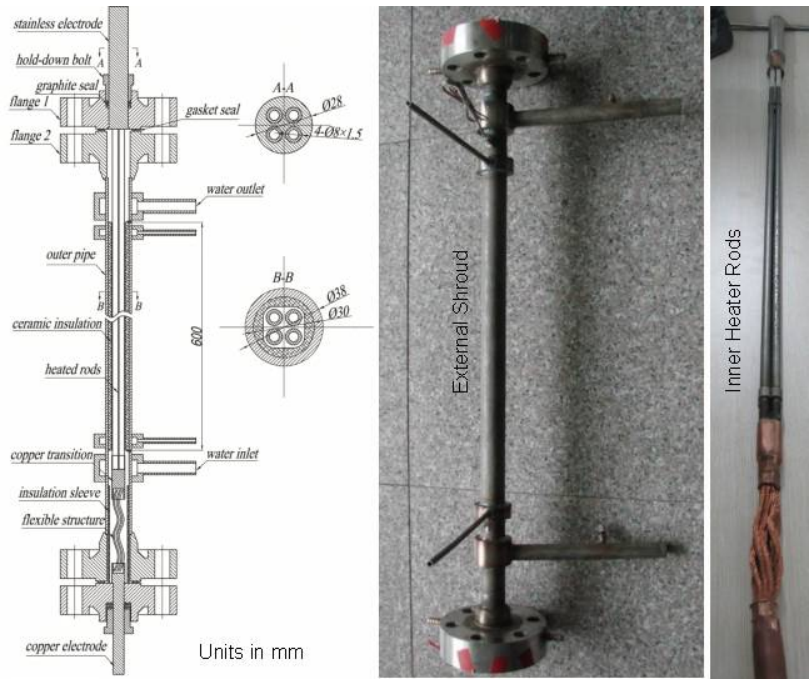

Figure 6: 2x2 Bundle Test-Section Configuration.

Two grid spacers, having the same outer dimensions as the ceramic insulator, were installed just outside of the heated section of the bundle to maintain the gap size between the heated rod and the ceramic insulator. No spacer was installed over the heated section, but the tubes were spot-welded

together at two locations to eliminate vibration when applying the AC current (see Figure 7 for the weld locations).

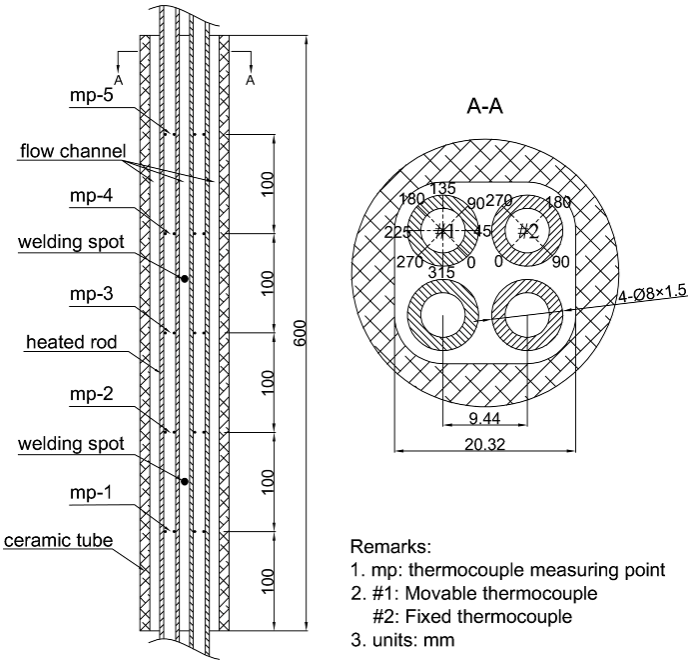

Figure 7: Thermocouple Measuring Points and Cross-Sectional Geometry of Flow Channel.

Wall-temperature measurements were obtained at two of the four heated tubes. Moveable thermocouples were inserted inside one of the tubes and fixed thermocouples were installed inside another tube. Figure 7 identifies the five locations (100-mm apart) covered by the moveable thermocouples along the heated tube. The moveable-thermocouples unit consisted of a probe carrying four standard NiCr-NiSi thermocouples (each wire with a 0.2-mm OD) with a circumferential interval of 90°. It was connected to a drive-assembly unit, which moved the probe axially and rotated the probe circumferentially inside the heated tube. At each location, the probe was rotated four times at an interval of 22.5° to measure the inner-wall temperatures (i.e., sixteen wall-temperature measurements along the circumference). Four fixed thermocouples were attached in a plane at 90° apart and inserted inside the other heated tube at the last measuring point covered by the moveable thermocouples (see Figure 7). These fixed thermocouples provided confirmatory measurements to the moveable thermocouples ensuring relatively consistent readings for all heated tubes.

Figure 8 illustrates the circumferential wall-temperature distribution around the heated tube at the pressure of 25 MPa, mass flux of 1000 kg/m^{2}s, surface heat flux of 400 kW/m^2, and inlet-fluid temperature of 417 °C (well beyond the pseudo-critical point). The presented wall temperatures correspond to outer-surface values calculated from inner-surface measurements obtained at the fifth thermocouple measuring point (mp-5). Wall temperatures at the corner region (around 180°) are higher than those in other regions. The increase in wall temperature at the corner region is attributed to the small gap with low flows and high enthalpies lowering the heat-transfer coefficient. The temperature gradient between the corner and the centre subchannel (where the lowest temperature is observed) regions is about 9 °C. This signifies that the wall temperature at the corner region increases more

rapidly than that at the centre subchannel region. Overall, the temperature variations from 0°-180° and from 180°-360° are relatively symmetrical. This signifies no tilting or bowing on the heated rod at this location. Measurements are similar between moveable and fixed thermocouples.

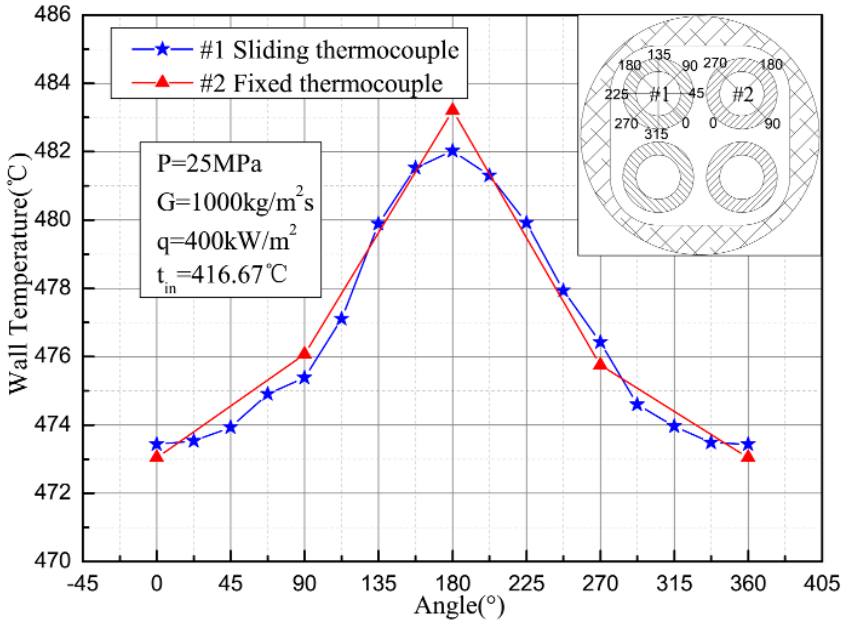

Figure 8: Circumferential Wall Temperature Distributions at Inlet-Fluid Temperature Higher Than the Pseudo-Critical Point.

Figure 9 shows the variations of maximum wall temperature around the circumference of the heated rod at the 5th measuring point with bulk enthalpy and heat flux at the pressure of 25 MPa and mass flux of 1000 kg/m^{2}s. In general, the maximum wall temperature increases with bulk-fluid enthalpy and heat flux. The leveling-off region at the vicinity of the pseudo-critical point is observed mainly at low heat fluxes and gradually becomes an increasing trend with increasing heat flux. It practically disappears at the heat flux of 800 kW/m^2. The trend is similar to those observed in tubes and annuli.

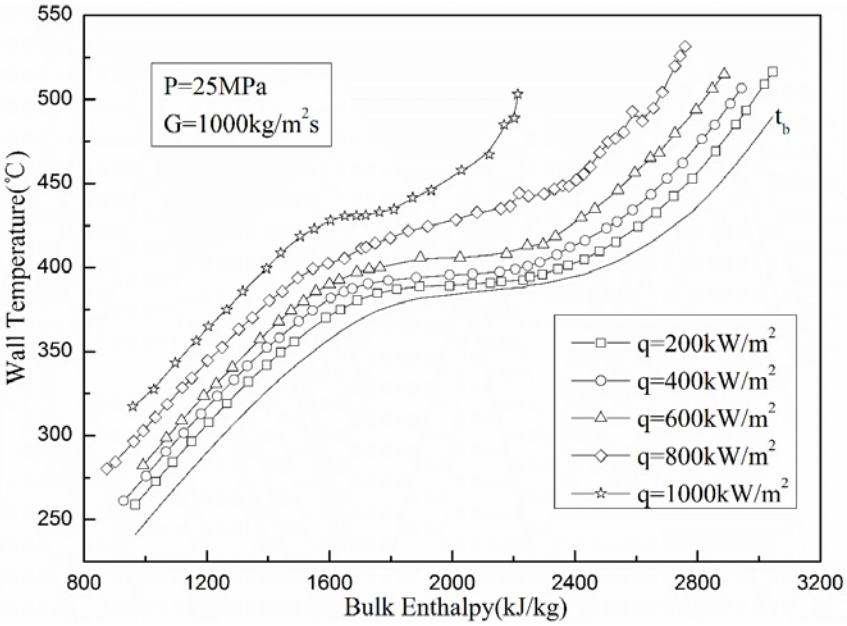

Figure 9: Variations of Maximum Wall Temperature with Bulk-Fluid Enthalpy and Heat Flux in a 2x2 Rod Bundle.

2.2 Supercritical Heat-Transfer Tests using Surrogate Fluids

Performing heat-transfer experiment with supercritical water flow is complex and expensive due primarily to the harsh operating environment. Surrogate fluids (such as carbon dioxide and refrigerants) have been used for modeling water in heat transfer studies. This approach is valid for improving the understanding of heat-transfer phenomena and examining separate effects. However, extending experimental results of surrogate fluids to water applications requires validated fluid-to-fluid modeling parameters.

2.2.1 Supercritical Carbon Dioxide Heat Transfer Test

A carbon-dioxide test facility has been constructed for supercritical heat-transfer experiments at University of Ottawa [10]. The loop is designed for a maximum pressure of 15 MPa and a nominal operating pressure of 10 MPa. It is filled with CO_2 from cylinders with an internal pressure of 13 MPa through a regulating valve. Two gear pumps have been installed to circulate the CO_2 flow through the loop. The flow rate in the loop is regulated by adjusting the pump speed using a single inverter. A DC power supply rated at a maximum voltage of 60V and a maximum current of 2833A provides the power through joules heating to the test section. An 8-mm ID tubular test section has been installed for commissioning and confirmatory experiments. Figure 10 illustrates the schematic diagram of the CO_2 flow loop and the set up of the 8-mm ID tubular test section.

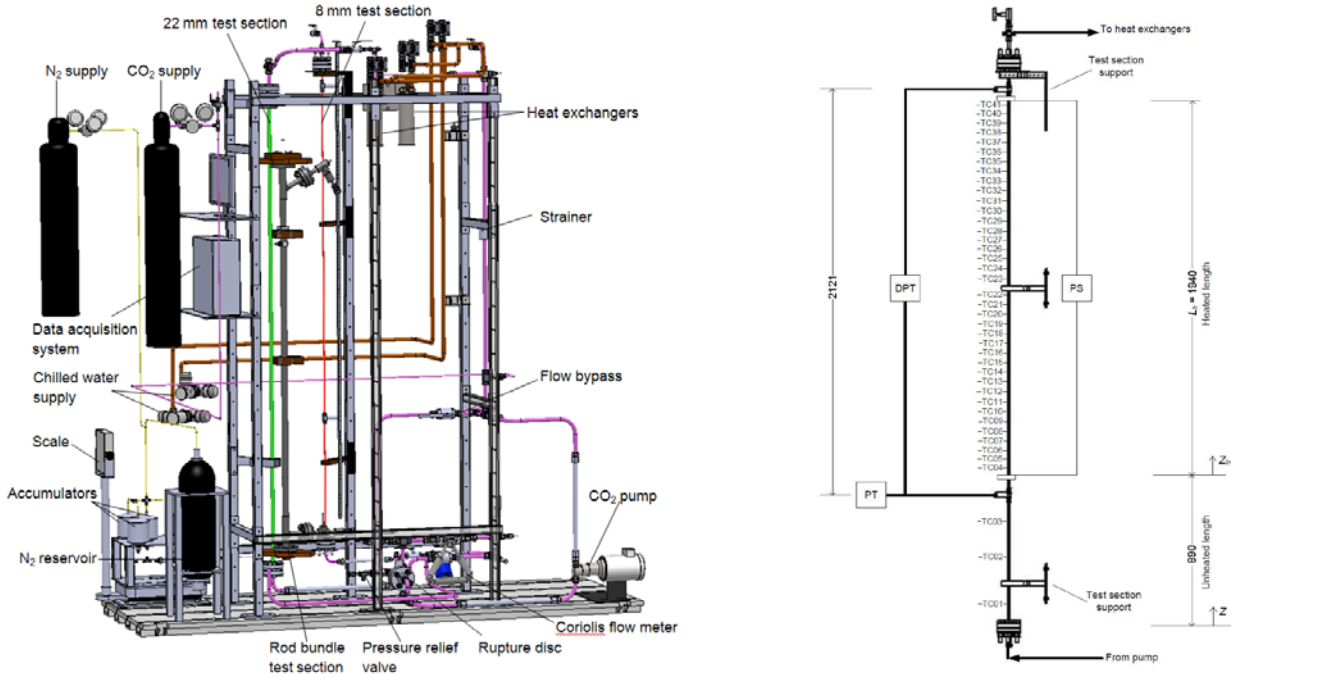

Figure 10: Schematic Diagram of the CO_2 Flow Loop and Tubular Test Section.

Supercritical heat-transfer experiments were performed using an 8-mm tubular test section covering a range of flow conditions (from subcritical to supercritical pressures) [11]. Figure 11 illustrates the axial surface temperature distribution along the test section. In general, the surface temperature increases with axial distance up to about 125 z_h/D, beyond which the surface temperature decreases. A sharp rise in surface temperature has been observed near the inlet of the heated section, signifying the deteriorated heat-transfer phenomena. The surface-temperature measurements were compared against those obtained in 2004 by Fewster and Jackson [12]. With a longer heated length in the current test section, more data points were collected in the current experiment than the experiment of Fewster and Jackson. Good agreement is shown in Figure 11 between these two set of data, especially over the deteriorated heat-transfer region. This enhances the confident on the current dataset and the experimental facility.

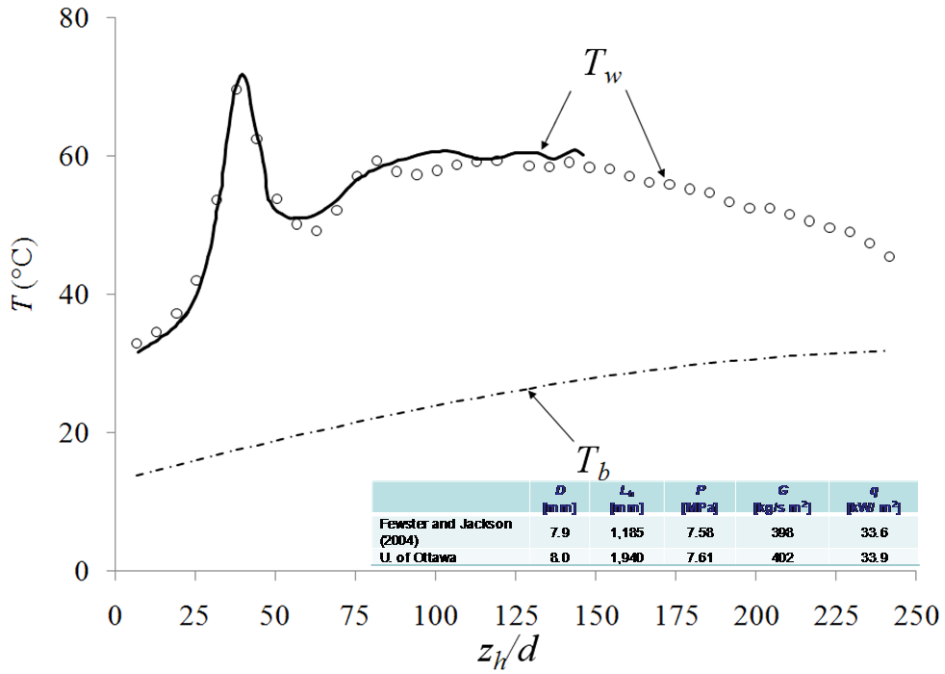

Figure 11: Surface Temperature Distribution along the CO_2 Cooled Vertical Tube.

Performing heat-transfer experiments using a 3-rod bundle is the main focus of the study at University of Ottawa. The test section consists of a pressure tube with an inner diameter of 25.4 mm (see Figure 12) and a Teflon tube acting as electric insulator between the heated bundle and the pressure tube.

The bundle was constructed with three 10-mm OD Inconel-600 tubes having a heated length of 1.5 metres. Each rod consisted of an unheated copper section at each end for connecting to the power bars. The spacing between rods was 1.4 mm, resulting in a pitch-to-diameter ratio of 1.14. It was maintained by wrapping a hypodermic stainless-steel tubing of 1.3 mm around each rod. To eliminate mal-distribution of flow in various subchannels, three unheated fillers were installed at the subchannels neighbouring to the pressure tube. Excluding the heated rod and the fillers, the flow area of the channel is 177 mm^2, with a corresponding hydraulic diameter of 6.7 mm. A moveable thermocouple assembly was installed inside each heated rod. It consisted of a carriage rod, near the upstream end of which two insulated K-type thermocouples are mounted across from each other. A loaded spring pushes each thermocouple against the heated surface to ensure good thermal contact. Each thermocouple may be rotated within the rod over 360° and traversed along the rod.

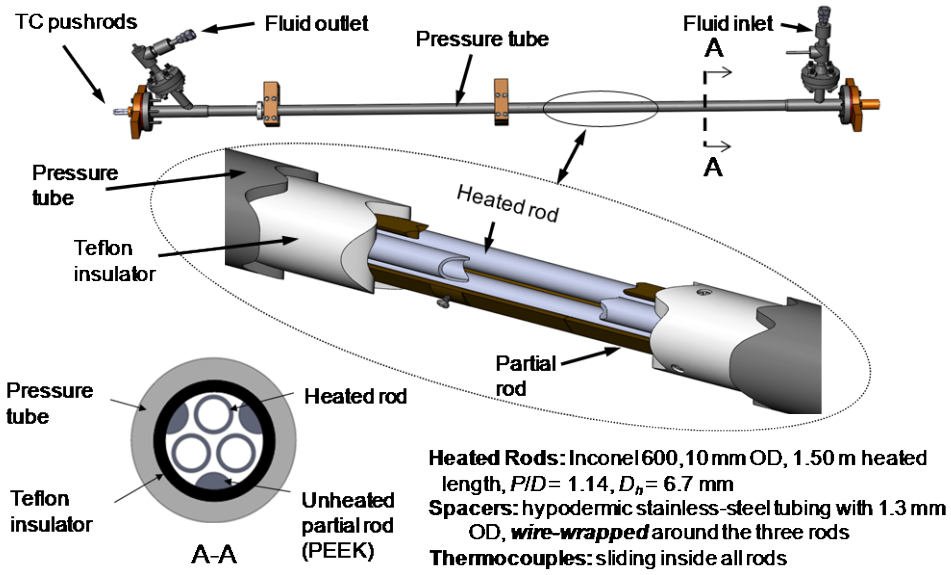

Figure 12: Schematic Diagram of the 3-Rod Bundle Test Section for the Supercritical CO_2 Experiment.

Figure 13 illustrates the circumferential wall-temperature distributions around the three heated rods at the axial location of 852.2 mm. Overall, the wall temperature variation is each rod is non-symmetry. The peak temperature appears to occur at surfaces facing the outer-subchannels neighbouring to the insert. The differences in wall-temperature distribution between rods are probably attributed to the wire-wrapped spacer locations. An extensive set of measurements have been obtained at various axial locations (from 30 to 1465 mm) taking advantages of the flexibility in using the moveable thermocouples. The experiment is in progress to cover other heat fluxes and flow conditions.

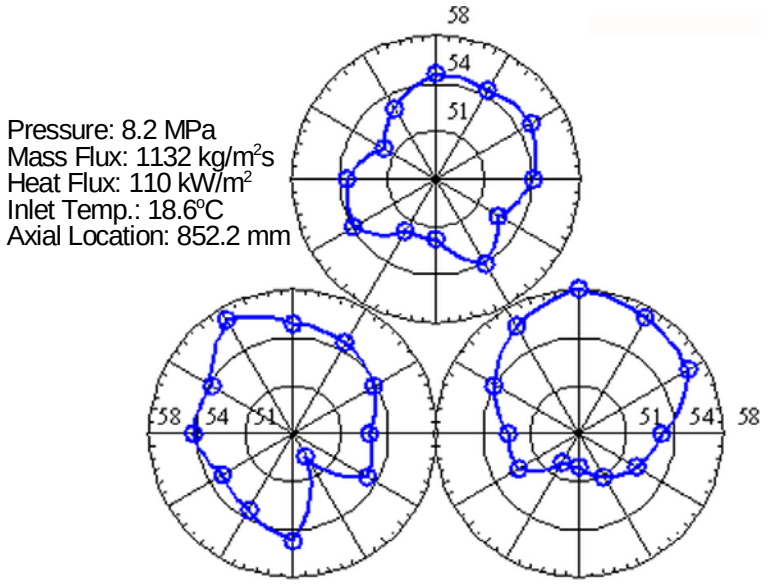

Figure 13: Preliminary Wall-Temperature Measurements from the Supercritical CO_2 Experiment with a 3-Rod Bundle.

2.2.2 Supercritical Refrigerant Heat-Transfer Test

A refrigerant test facility has been constructed for supercritical heat-transfer experiments at Carleton University [12]. The loop is designed for a maximum pressure of 6 MPa and temperature of 140°C. While various types of refrigerant can be accommodated in the loop, refrigerant-134a (or R-134a) has been adopted currently as the working fluid. Refrigerant flow is driven by three gear pumps, connected in parallel. The flow rate is measured using a turbine flow meter.

Three test sections have been constructed for the experiment: tubular, annulus, and 7-rod cluster. These test sections were designed for testing in both water and refrigerant flows. The tubular test section was constructed with an Inconel-625 tube having an inside diameter of 12.5 mm and a wall thickness of 3.5 mm. Two power clamps were attached to the test section resulting in a heated length of 2 meters. The test section was instrumented with N-type thermocouples on the outer surface of the tube at a 10-mm increment.

Figure 14 illustrates the variations of surface temperature measurement with bulk-fluid enthalpy and heat flux at the pressure of 4.3 MPa, mass flux of 600 kg/m^{2}s and inlet-fluid temperature of 10°C. The surface temperature increases with heat flux. It increases with increasing bulk-fluid enthalpy at the heat flux of 21.6 kW/m^2. A localized sharp rise in surface temperature has been observed at bulk-fluid enthalpies of 230 kJ/kg and 220 kJ/kg for the heat fluxes of 33 kW/m^2 and 58.2 kW/m^2, respectively. This signifies the deteriorated heat-transfer phenomena at those conditions.

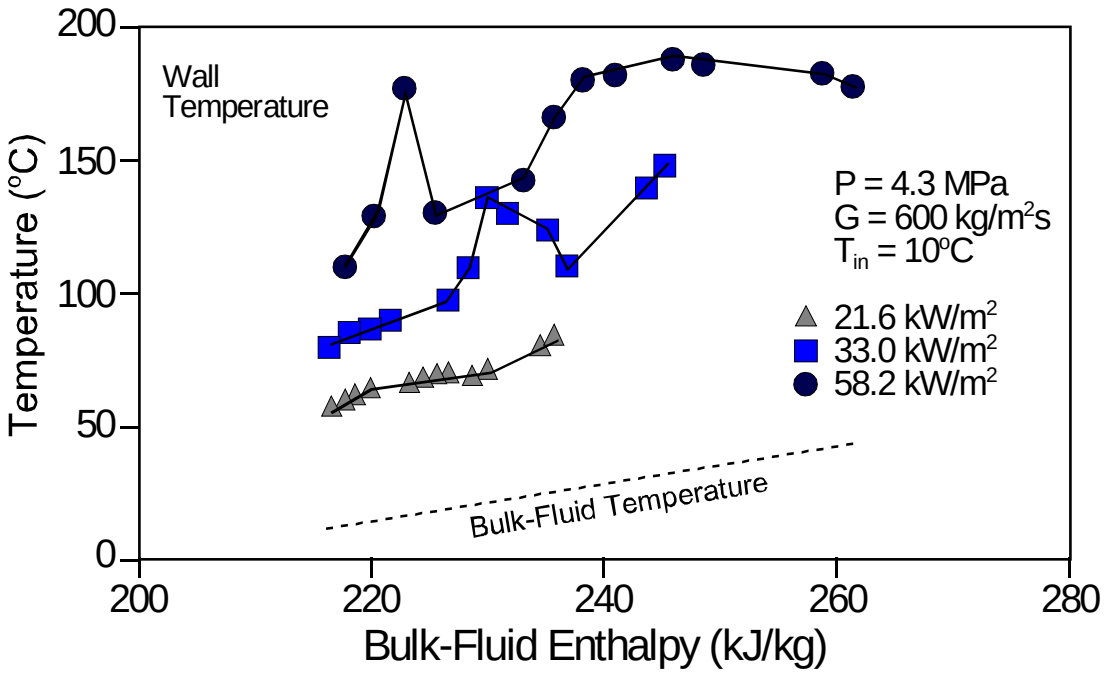

Figure 14: Surface Temperature Measurements along the Rerigerant-134a Cooled Vertical Tube.

The annulus test section consists of an inner heated Inconel-625 tube of 10-mm outer diameter with a wall thickness of 2.5 mm and an outer unheated Inconel-625 tube of 18-mm inner diameter (see Figure 15). It has a heated length of 2.244 meters. A moveable-thermocouples assembly was installed inside the inner heated tube to measure the inner-wall temperature distribution. Four sets of discrete

spacers were attached along the heated tube at locations of 85 mm, 856 mm, 1122 mm (mid point) and 2105 mm. These spacers maintained the heated tube at the centre of the pressure boundary, and held down the stainless-steel (SS316) wire wrapped around the heated tube. The wire has an outer diameter of 1.2 mm. Two wire pitches (100 mm and 200 mm) were tested in the experiment.

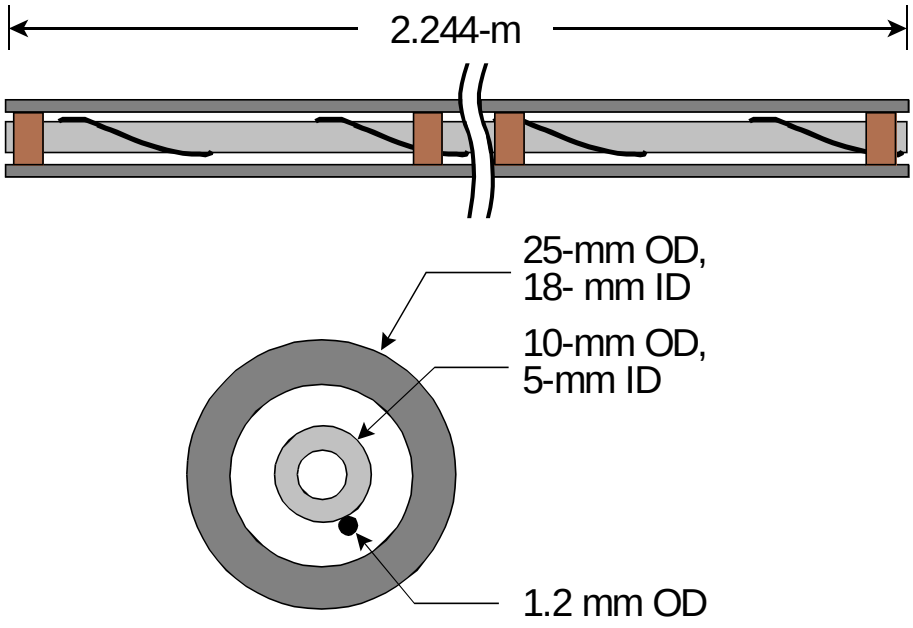

Figure 15: Schematic Diagram of the Wire-Wrapped Annular Test Section for Supercritical Refrigerant Experiments.

Figure 16 compares the experimental Nusselt numbers calculated from wall-temperature measurements along the annular test section with and without the wrapped wire for two mass fluxes. The Nusselt number is larger at the mass flux of 1300 kg/m^{2}s than of 600 kg/m^{2}s. Large localized disturbances in Nusselt number are shown at four locations of the discrete spacer. The enhancement effect of these spacers appears to have impact over a short downstream distance, particularly at the mass flux of 600 kg/m^{2}s. The installation of a wrapped wire along the heated rod has led to increases in Nusselt number (i.e., heat transfer enhancement) compared to that of a no-wire rod. Reducing the wire pitch from 200 to 100 mm increases further the Nusselt number, but the difference is relatively small.

3. Recent Safety-Related Experiments with Supercritical Flow

Improved safety is one of the technology goals for the Gen-IV nuclear-reactor systems. Experimental data and analytical models are needed to support the design of the SCWR and to ensure that any new phenomena introduced as a result of using supercritical water are understood.

3.1 Stability and Natural Circulation

Large variation of coolant density in the axial direction and strong coupling of the neutronic and thermal-hydraulic behavior makes the system theoretically susceptible to dynamic oscillations. This instability may lead to high cladding temperature in the fuel prematurely impacting on the operating and safety margins. Susceptibility to dynamic instability has been evaluated only for one-dimensional single-channel steady-state operating conditions. Parallel-channel (out-of-phase) instabilities as well as

instabilities that might arise during start-up, coast-down, and power transients have not been investigated.

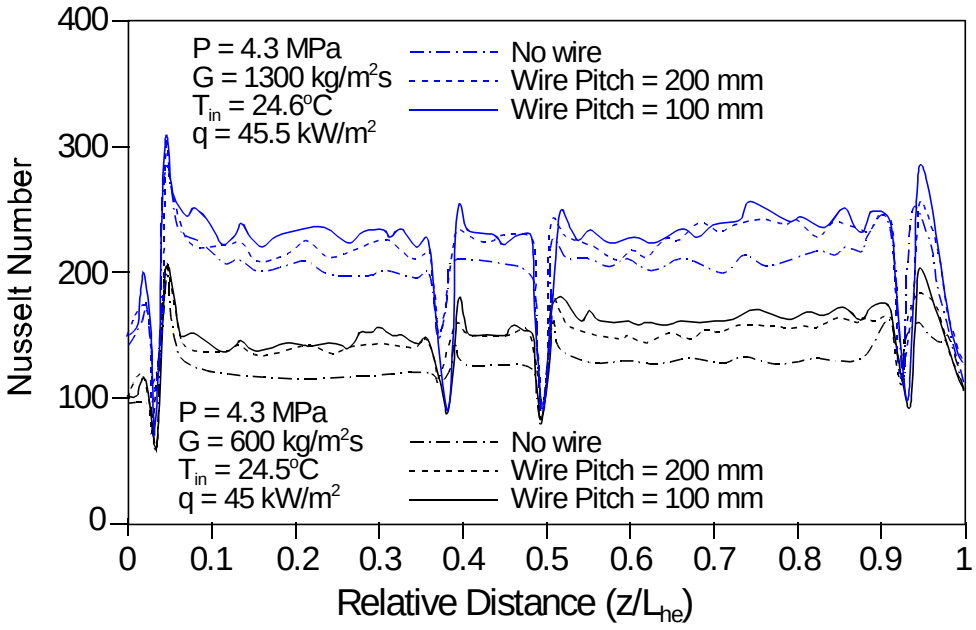

Figure 16: Experimental Nusselt Number along the Annular Test Section with or without Wrapped Wire.

Analytical models have been developed to establish the stability region in support of the SCWR design. These models can be applied to examine one-dimensional in-phase oscillations and two- and three-dimensional out-of-phase oscillations. Validation of these models is required against experimental data obtained at supercritical conditions.

A separate CO_2 test facility has been constructed for natural circulation and stability experiments at University of Manitoba [14]. The loop is designed for a maximum pressure of 12 MPa, and outlet temperature of 95°C. It is constructed with stainless steel 316L pipes, tees and elbows. Four ball valves were welded to the loop for controlling the flow rate through the test section. Six fluid thermocouples (Type K) were also installed at various locations on the experimental facility to measure bulk fluid temperatures.

A pressure control system was designed to maintain a constant loop pressure (see Figure 17). The system consists of a single stage pressure regulator connected to a nitrogen gas bottle and to an accumulator. The bladder accumulator consists of a fluid section (working fluid) and a gas (nitrogen gas) section where the bladder acts as a gas-proof screen in the accumulator.

The test section consists of an Inconel-625 tube (¾-in I.D. and 0.508-in thick) connected to inlet and outlet headers (see Figure 18). It is heated with a DC power supply with maximum current capacity of 1500A at maximum voltage of 20 volts. Twelve surface thermocouples (Type K) are attached to the outer surface of the channel. An electro-pneumatic valve is installed upstream of the inlet header and downstream of the outlet header. Each electro-pneumatic valve assembly consists of a valve, pneumatically controlled actuator and a position controlling transducer.

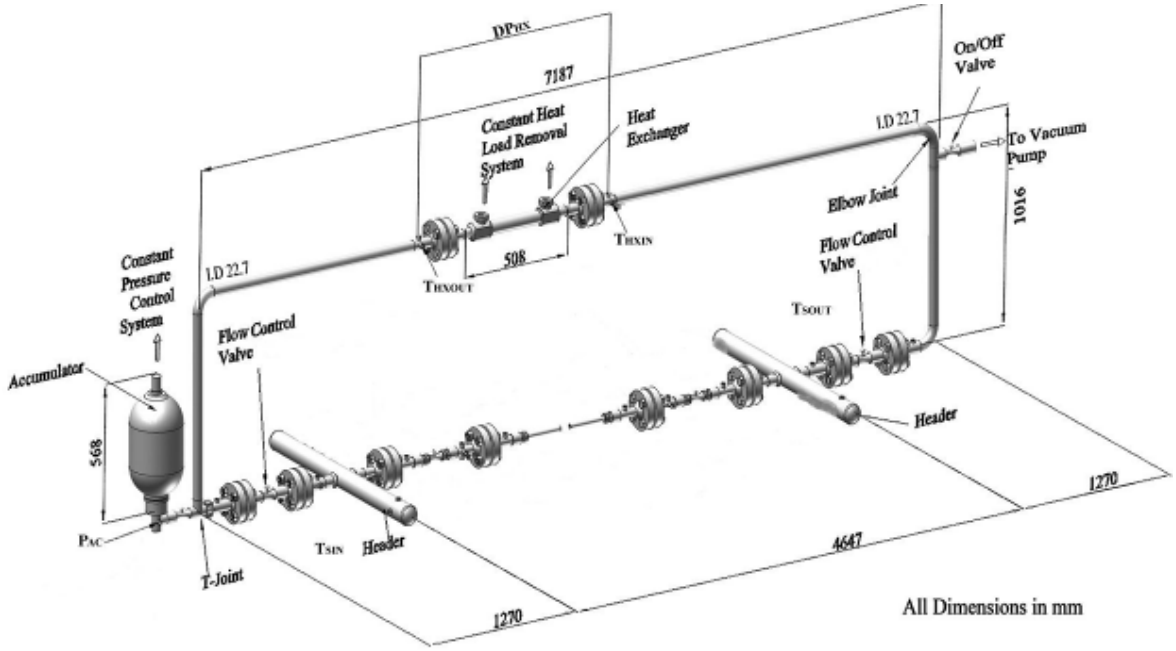

Figure 17: Schematic Diagram of the Natural Circulation and Stability Test Facility.

A shell and tube micro-heat-exchanger is installed to remove heat from the primary system. Differential pressure transducers are used to measure the pressure drop across four electro-pneumatic valves and two headers, and across the channel and across the heat exchanger. Three absolute pressure transducers are used to measure the absolute pressures in the accumulator and in the inlet and outlet headers of the test section.

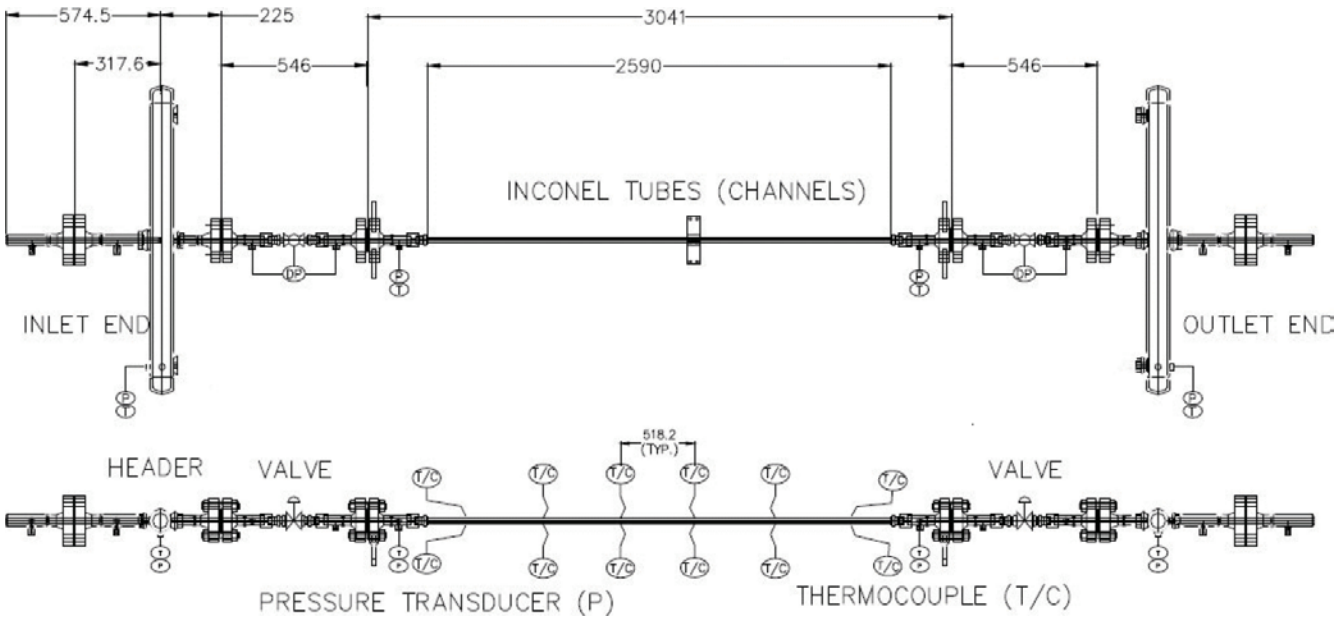

Figure 18: Test Section Setup for the Natural Circulation and Stability Test

Natural circulation tests were performed over a range of powers [13]. Measured mass flow rates and corresponding frictional pressure drops are shown in Figure 19 for two configurations of valve operation at the inlet and outlet of the test section. The mass flow rate increases when raising the power applied to the test section. The increase is steeper at low powers than at high powers. Correspondingly, the frictional pressure drop across the test section increases with increasing power. The increasing trend is relatively linear over the current range.

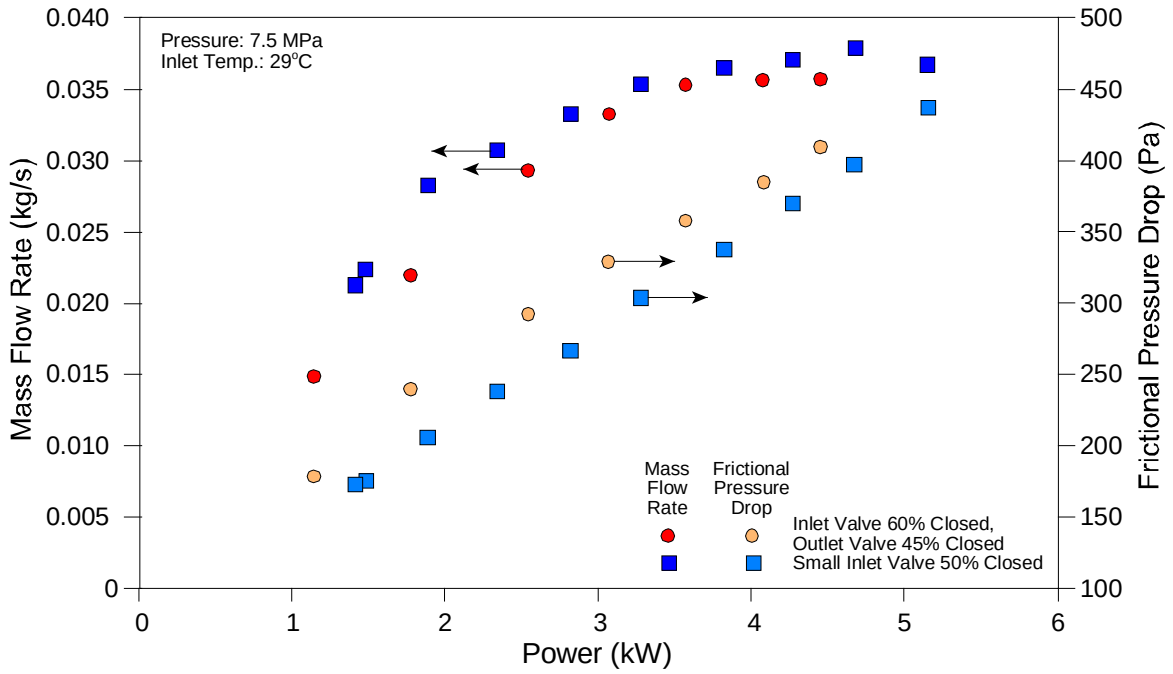

Figure 19: Variations of Mass Flow Rate and Pressure Drop in Natural Circulation Test

The valve-closing configuration affects the pressure drop of the system and hence the mass flow rate. As shown in Figure 19, the pressure drop is larger with the inlet and outlet valves closed at 60% and 45%, respectively, than with the small inlet valve closed at 50% at the same power level.

Corresponding, the mass flow rate is slightly higher when closing the small inlet valve by 50% than when closing the inlet and outlet valves by 60% and 45%, respectively. The outlet temperature reaches 39°C when both valves were closed and 40°C when the small inlet valve was closed, exceeding the pseudo-critical temperature. In both cases, no flow instability was encountered but thermo-acoustic high frequency oscillations were observed during the experiments.

3.2 Critical Flow Test Facility using Water as Working Fluid

Critical (or choked) flow phenomena are of great importance in designing and operating the reactor safety (or relief) valves and the automatic depressurization system during normal operation. Understanding these phenomena also facilitates the analysis of a large-break loss-of coolant event. Most critical-flow studies were performed at subcritical conditions in support of the design and safety analyses of light-water reactors. Experimental data obtained from those studies were used to develop critical-flow models. Strictly speaking, these models are applicable for subcritical conditions only and extending to supercritical conditions is not justifiable due to their empirical nature. Critical-flow

models can be extended to supercritical applications through benchmarking against experimental data. However, a literature review has concluded the lack of critical-flow data at supercritical conditions. A supercritical water loop has been constructed to carry out supercritical critical flow experiments at Ecole Polytechnique de Montreal. A schematic diagram is shown in Figure 20. The loop is connected to an existing main steam-water loop of medium pressures, where the supercritical water is discharged into. It consists of a cooler, a water filter system, a high pressure volumetric pump, a pulsation dampener, a heater, a flow stabilization plenum, a test section and a flow discharge chamber. The loop is designed for maximum pressure of 260 bar (abs), temperature of 625 °C, and flow rate of 0.15 litre/s.

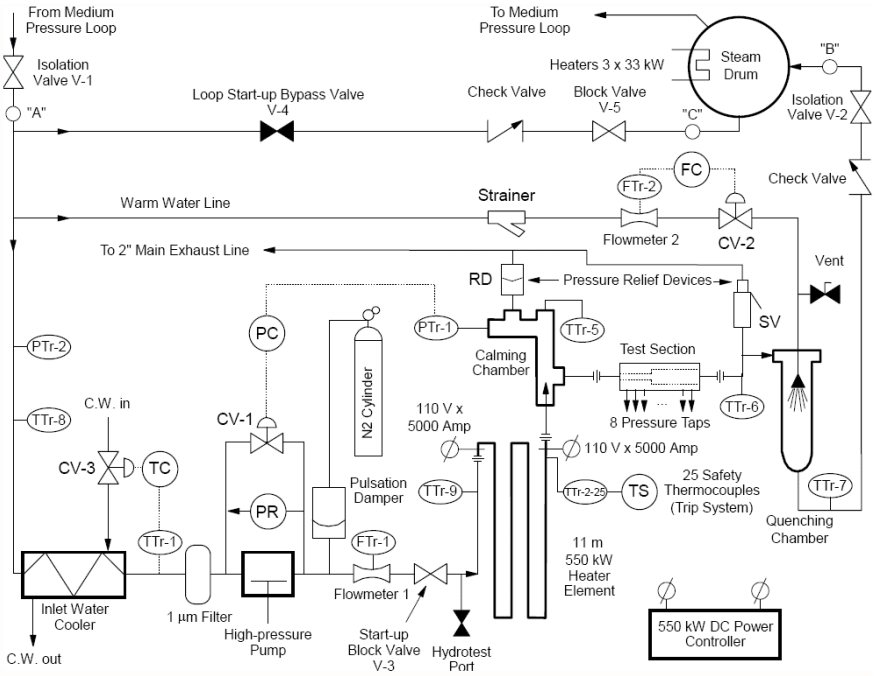

Figure 20: Supercritical-Water Loop for Critical-Flow Experiment

The system is pressurized using a high-pressure nitrogen supply together with a pulsation dampener system to reduce pulsations and hydraulic shocks. A needle-type bypass valve is initially used for maintaining the pressure constant during the experiments. This valve is controlled automatically by using an appropriate control unit. The pressure control system is combined with a supplementary variable speed motor controller to provide fine pressure adjustment.

A six-plunger pump is installed to circulate the fluid. A cooler is installed upstream of the pump inlet to reduce the fluid temperature to the acceptable level (less than 70°C). The fluid is heated with heater elements to the desirable temperature prior to entering the test section. It is then discharged into a chamber, which is connected to the medium pressure loop. The pressure in the chamber is adjustable and controllable. It is measured using an absolute pressure transducer.

The test section consists of a 1-mm ID, 3.2-mm long, opening connecting two chambers of larger diameter (nozzle). Fluid in the upstream chamber is maintained at supercritical conditions. Figure 21 illustrates the nozzle design in the discharge chamber. The square nozzle would lead to an abrupt discharge of the fluid to the chamber, while the cone-shape nozzle results in a gradual discharge.

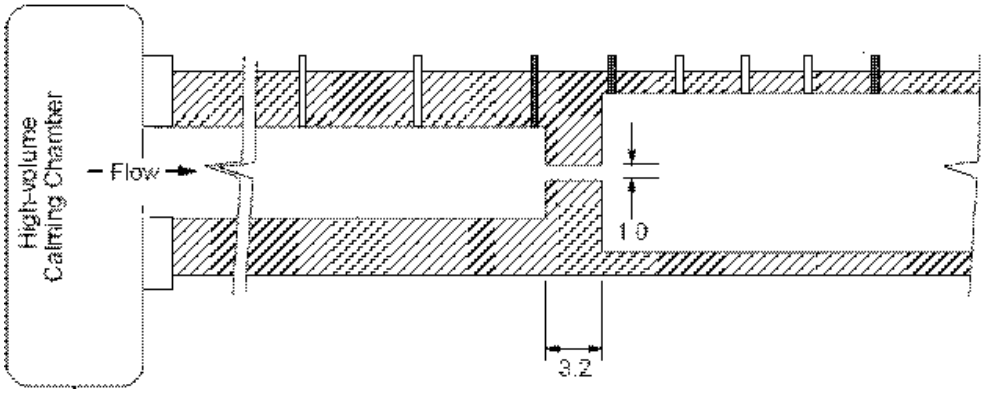

Figure 21: Sharp-Edge Nozzle at the Discharge Chamber of the Critical-Flow Test Facility.

Eight pressure taps have been installed to establish the pressure distribution over the nozzle region. Three of these taps are located in the small-diameter section and the other taps in the discharge chamber (i.e., expansion region). Differential pressure transducers have been installed to measure pressure losses over these taps, which are used to establish the axial pressure distribution at the straight small-diameter section and the discharge chamber.

Figure 22 illustrates the variations of critical mass fluxes with temperature and pressure at the calming chamber upstream of the square-discharged nozzle (see Figure 21). Expressing the upstream temperature in term of the temperature difference with the pseudo-critical temperature, the critical mass flux increases with increasing temperature difference. Some scatters among the critical mass flux have been observed at the pseudo-critical temperature (i.e., ΔT_{pc}). The effect of pressure appears small over the current range.

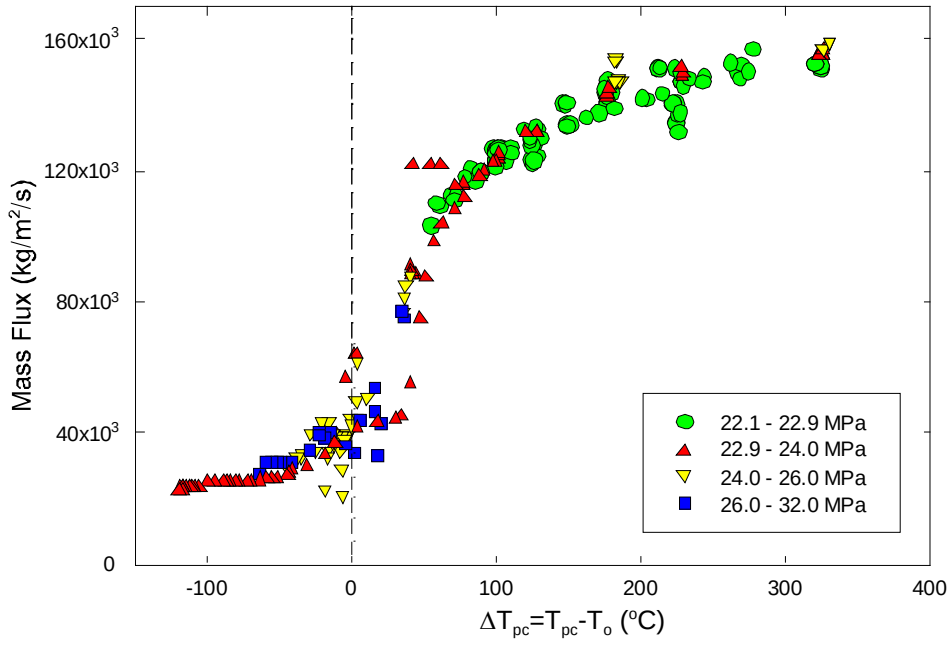

Figure 22: Variations of Critical Mass Fluxes with Temperatures and Pressures at the Calming Chamber (i.e., Inlet of the Nozzle).

4. Conclusions

- An extensive thermalhydraulics program has been established to support the development of the Canadian SCWR concept.
- New experimental heat-transfer data have been obtained with water, carbon dioxide, and refrigerant-134a flow in tubes, annuli, and bundle subassemblies.
- These data facilitate improvement in understanding of heat-transfer characteristics to fluids at supercritical pressures.
- These data are ideal for verification of prediction methods and analytical tools.

5. Acknowledgment

The author would like to thank the support of Office of Energy Research and Development (OERD) at Natural Resources Canada and the Natural Sciences and Engineering Research Council (NSERC) of the Canadian Gen-IV National Program. Contributions from Prof. Tavoularis at University of Ottawa, Prof. Yaras at Carleton University, Prof. Chatoorgoon at University of Manitoba, Prof. Teyssedou at Ecole Polytechnique de Montreal, and Prof. Bi at Xi'an Jiaotong University are appreciated.

6. References

[1] Preville, M., Sadhankar, R., Brady, D., "Canada's National Generation IV Program", Proc. 28th Annual CNS Conference, Saint John, NB, Canada, June 3-6, 2007.

[2] M.E. Shitsman, Impairment of the heat transmission at supercritical pressures, High Temperature 1 (1963) 237–244.

[3] A.A. Bishop, R.O. Sandberg, L.S. Tong, Forced convection heat transfer to water at near critical temperatures and supercritical pressures. WCAP-2056-P, Part-III-B, 1964.

[4] H.S. Swenson, J.R. Carver, C.R. Karakala, Heat transfer to supercritical water in smooth-bore tubes, J. Heat Transfer, Trans. ASME Ser. C 87 (1965) 477-484.

[5] K. Yamagata, K. Nishikawa, S. Hasegawa et al., Forced convective heat transfer to supercritical water flowing in tubes, Int. J. Heat Mass Transfer 15 (1972) 2575-2593.

[6] J. Licht, M. Anderson, M. Corradini, Heat transfer to water at supercritical pressures in a circular and square annular flow geometry, Int. J. Heat Fluid Flow, 29 (2008) 156-166.

[7] G. Wu, Q.C. Bi, Z.D. Yang, et al., Experimental investigation of heat transfer for supercritical pressure water flowing in vertical annular channels, Nucl. Eng. Des. 241 (2011) 4045-4054.

[8] H. Mori, T. Kaida, M. Ohno, et al., Heat transfer to a supercritical pressure fluid flowing in sub-bundle channels. Journal of Nuclear Science and Technology. 49 (2012) 373-383.

[9] Zhao, M., Li, H.B., Yang, J., Gu, H.Y. and Cheng, X., "Experimental study on heat transfer to supercritical water flowing through circular tubes and 2×2 rod bundles", Proceeding of the 6th International Symposium on Supercritical Water-cooled Reactors, Shenzhen, China, March 3-7, 2013.

[10] Jeddi, L., Jiang, K., Tavoularis, S. and Groeneveld, D.C., "Preliminary Tests at the University of Ottawa Supercritical CO_2 Heat Transfer Facility", Proc. 5th Int. Sym. SCWR (ISSCWR-5), Vancouver, British Columbia, Canada, March 13-16, 2011.

[11] Zahlan, H., Jiang, K., Tavoularis, S. and Groeneveld, D.C., "Measurements of Heat Transfer Coefficient, CHF and Heat Transfer Deterioration in Flows of CO_2 at Near-Critical and Supercritical Pressures", Proceeding of the 6th International Symposium on Supercritical Water-cooled Reactors, Shenzhen, China, March 3-7, 2013.

[12] Fewster, J. and J.D. Jackson, "Experiments on Supercritical Pressure Convective Heat Transfer Having Relevance to SCWR", Proc. ICAPP'04, Paper 4342, Pittsburgh, PA, USA, June 13−17, 2004.

[13] Balouch, M. and Yaras, M.I., "Design of an R-134a Loop for Subcritical and Supercritical Forced-Convection Heat Transfer Studies", Proc. International Conference on Future of Heavy Water Reactors, Ottawa, Ontario, Canada, Oct. 02-05, 2011.

[14] Mahmoudi, J., Chatoorgoon, V. and Leung, L., "Experimental Thermal-hydraulic Analysis of Supercritical CO_2 Natural Circulation Loop", Proc. 33rd CNS Annual Conf./36th Annual CNS/CNA Student Conference, Saskatoon, Saskatchewan, Canada, June 10 – 13, 2012.